

Morphology-Preserving Conversion of a 3D Bioorganic Template into a Nanocrystalline Multicomponent Oxide Compound**

Jonathan P. Vernon, Yunnan Fang, Ye Cai, and Kenneth H. Sandhage*

The development of a robust process for generating functional assemblies possessing complex (three-dimensional, 3D) morphologies with well-controlled patterns of fine (micro-to-nanoscale) features along with complex (multicomponent) and tailorable inorganic compositions remains a considerable challenge. One strategy for such versatile fabrication is to convert a 3D micro/nanostructured solid template, generated through a biological or synthetic self-assembly process, into a new inorganic composition by a morphology-preserving chemical transformation process; that is, to decouple the 3D template formation and chemical tailoring processes.^[1] The purpose of this paper is to introduce a broadly applicable bottom-up approach for chemical conversion of intricate 3D nanostructured (bio)organic templates into positive replicas comprised of multicomponent oxide compounds. This general process consists of the following steps: 1) the generation of a thin conformal coating on a 3D (bio)organic template by a layer-by-layer (LbL) process, 2) pyrolysis of the template and collapse of the thin coating into the space previously occupied by the prior solid (bio)organic material, and 3) conversion of the resulting inorganic structure into a nanocrystalline multicomponent oxide compound by a low-temperature hydrothermal reaction. This work reveals, for the first time, how a 3D (bio)organic template may be converted into a positive replica comprised of a nanocrystalline multicomponent oxide compound by coupling the precise structural (sub-nanometer) and versatile chemical control of conformal coatings provided by an automated surface sol-gel (SSG) process^[2] with the low-temperature compound formation provided by microwave hydrothermal (MWHT) processing.^[3] To our knowledge, no prior report exists of the use of hydrothermal processing to convert conformally coated intricate 3D organic structures into functional multicomponent oxide replicas.

This shape-preserving process has been demonstrated by converting the 3D micro/nanostructured wing scales of a *Morpho helenor* butterfly into tetragonal barium titanate (BaTiO_3) replicas. *M. helenor* wing scales are comprised of a

natural polysaccharide, chitin, that contains an abundance of hydroxy groups for reaction with metal alkoxide precursors used in the SSG process.^[2d,4] Barium titanate was selected as a representative multicomponent oxide product owing to the extensive use of compositions based on this perovskite compound in a variety of applications (e.g., multilayer capacitors, thermistors, microwave dielectrics).^[5]

Secondary electron (SE) images revealing the morphology of the scales present on the brown side of a female *M. helenor* butterfly are shown in Figure 1a. As seen in the lower magnification inset image, the scales possess an overall rectangular shape with pointed tips. The higher-magnification image reveals parallel ridges that are aligned with the long dimension of the scale. Adjoining ridges are spaced several micrometers apart and are connected by perpendicular struts. The scales also contain parallel ribs spaced about 150 nm apart. Thin, conformal, and continuous titania-bearing coatings were applied to these nanostructured scales in a computer-controlled LbL SSG process. Each cycle of this process involved exposure to a titanium(IV) isopropoxide solution in anhydrous isopropyl alcohol (IPA), washing with IPA, exposure to a solution of 40 vol % IPA in water, washing again with IPA, and then drying with warm flowing nitrogen.

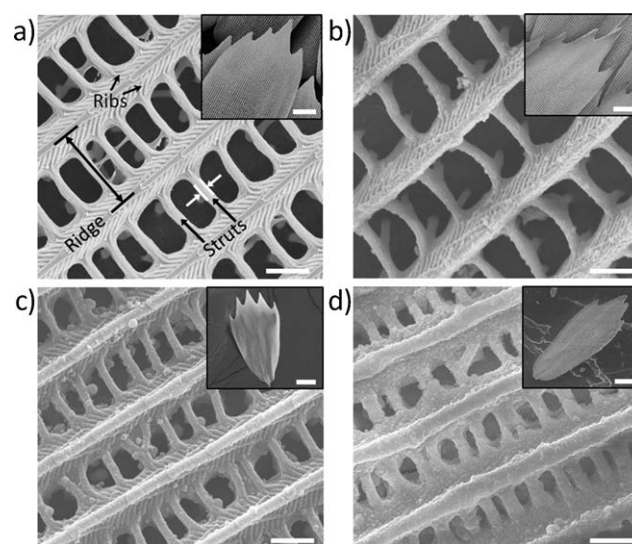


Figure 1. Secondary electron (SE) images of scales from the brown side of a female *Morpho helenor* butterfly wing at various stages of conversion: a) a chitinous starting scale, b) an as-coated scale after 51 SSG deposition cycles, c) a SSG coated scale after organic pyrolysis, and d) a SSG coated and pyrolyzed scale after MWHT conversion into BaTiO_3 . Insets are lower magnification images of the same scales showing overall morphological retention. Scale bars: 1 μm (high-magnification images), 20 μm (inset images).

[*] J. P. Vernon, Dr. Y. Fang, Dr. Y. Cai, Prof. Dr. K. H. Sandhage
School of Materials Science and Engineering
Georgia Institute of Technology
771 Ferst Drive, Atlanta, GA 30332-0245 (USA)
Fax: (+1) 404-385-3436
E-mail: ken.sandhage@mse.gatech.edu

[**] This work was supported by the Air Force Office of Scientific Research (Dr. Hugh DeLong, program manager) and the Office of Naval Research (Dr. Mark Spector, program manager). We acknowledge the Georgia Tech FIB2 Center established under NSF funding.

Supporting information for this article is available on the WWW under <http://dx.doi.org/10.1002/anie.201003170>.

This automated process was repeated for a total of 51 cycles. The coated scales were then heated at $0.5^{\circ}\text{Cmin}^{-1}$ to 450°C and held at this temperature for 4 h in air to allow for pyrolysis of the chitin. The resulting oxide-based structures then underwent MWHT reaction with a basic, barium acetate-containing aqueous solution at 220°C for 10 h to allow for conversion into nanocrystalline tetragonal BaTiO_3 (note: similar MWHT conditions have been used to convert hydrous titania powder into tetragonal barium titanate^[3b]).

SE images of scales at various stages of conversion are shown in Figure 1 a–d. The overall scale morphology, parallel ridges, and perpendicular struts were retained in the as-coated, pyrolyzed, and hydrothermally reacted scales. Confocal Raman spectroscopic analyses of as-coated scales (as shown in Figure 2 b), and selected area electron diffraction (SAED) analyses of focused ion beam (FIB) milled cross-

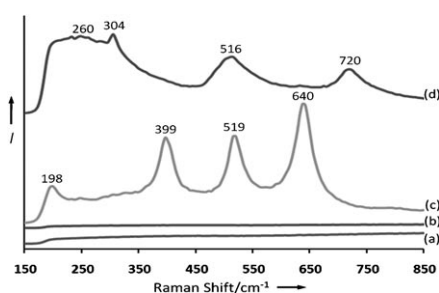


Figure 2. Raman spectra obtained from *M. helenor* scale samples at various stages of conversion: a) a chitinous starting scale, b) an as-coated scale after 51 SSG deposition cycles, c) a SSG coated scale after organic pyrolysis, and d) a SSG coated and pyrolyzed scale after MWHT conversion into BaTiO_3 . The number shown above each peak corresponds to the wavenumber at which the maximum peak intensity was measured.

sections (not shown), indicated that the coating was amorphous. After organic pyrolysis, however, Raman analyses of coated scales (Figure 2 c) yielded peaks consistent with anatase titania.^[6a] High-magnification SE images (Supporting Information Figures S1c, S2a), TEM/SAED analyses (Figure 3 a and c), and lattice fringe images obtained from high-resolution transmission electron microscopy (HRTEM) of FIB-milled cross-sections (Figure 3 e) indicated that the coating was comprised of nanocrystalline anatase titania (note: the 0.352 nm and 0.243 nm values of lattice fringe spacing shown in Figure 3 e correspond to the (101) and (103) spacings, respectively, of anatase TiO_2). After MWHT reaction with barium acetate, high-magnification SE analysis (Figures S1d, S2b), TEM/SAED analyses (Figure 3 b and d), and lattice fringe images obtained from HRTEM of coating cross-sections (Figure 3 f) indicated that the titania had been converted into nanocrystalline BaTiO_3 (note: the 0.283 nm value of lattice fringe spacing shown in Figure 3 f corresponds to the (110) spacing of BaTiO_3). Raman analyses (Figure 2 d) also yielded peaks consistent with the tetragonal polymorph of barium titanate (note: the peaks centered at about 304 and 720 cm^{-1} have been reported to vanish upon heating above the BaTiO_3 Curie temperature).^[6b]

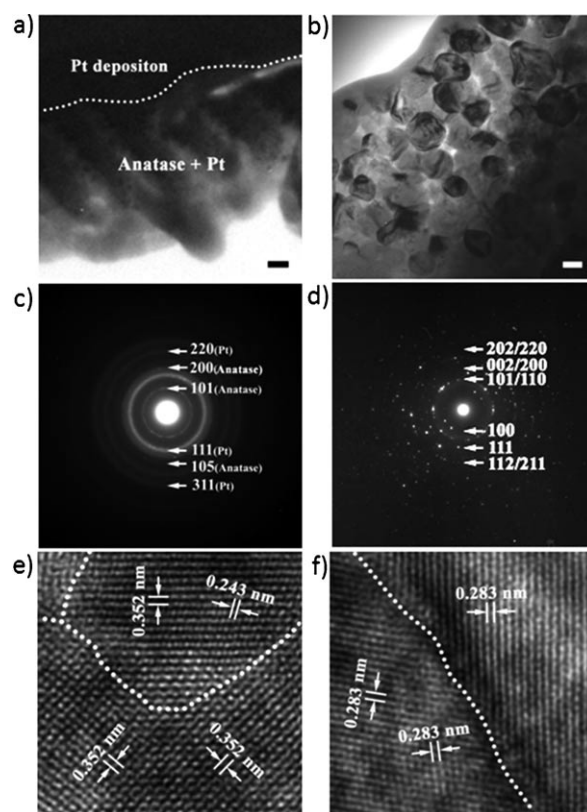


Figure 3. a,b) Bright field TEM images, c,d) corresponding SAED patterns, and e,f) HRTEM images of FIB milled cross-sections of TiO_2 (left column) and BaTiO_3 (right column) scale replicas. Note: 002/200 peaks in (d) are labeled together due to the proximity of these reflections. Scale bars: 50 nm.

To evaluate the 3D internal structures of the specimens at various stages of conversion, FIB milling was used to generate trenches within the scales, as shown in the SE images of Figure 4 a–d. These images of FIB-milled regions revealed similar internal morphologies (i.e., vertical struts supporting horizontal struts) for the natural, as-coated, pyrolyzed, and MWHT-reacted specimens. However, certain dimensional changes were detected at various stages of conversion. Measurements of the average strut width and ridge spacing (illustrated in Figure 1 a) are shown in Table 1. While no significant change in the ridge spacing was observed after application of the SSG coating, an average increase of about 65 nm was detected in the strut width, which was consistent with a sub-nanometer increase in coating thickness per SSG cycle. For further evaluation of the SSG coating morphology, the chitin template was removed by treatment in an oxygen plasma. High-resolution SE images of cross-sections of a ridge and a vertical strut of such a coated/plasma treated scale are shown in Figures S1a and S1b, respectively. The continuously-coated, chitin-free ridges and struts possessed hollow cores, which indicated that the alkoxide precursor did not penetrate deeply into the chitin during the SSG coating process. After thermal pyrolysis and conversion into nanocrystalline titania at 450°C , a noticeable decrease in the total scale thickness occurred (compare Figure 4 c and b). The average ridge spacing and the average strut width also decreased signifi-

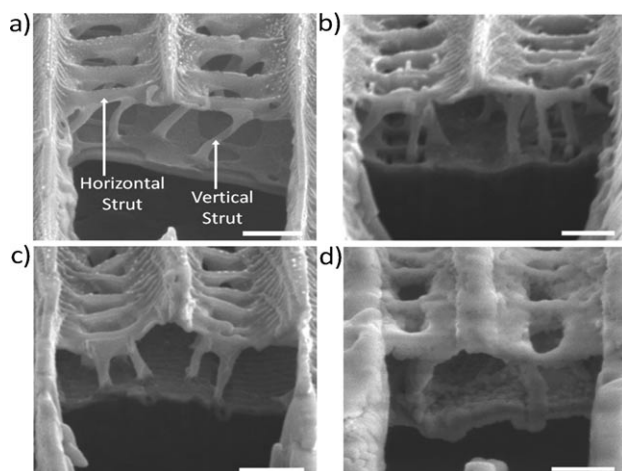


Figure 4. SE images of cross-sections of *M. helenor* butterfly wing scales, after FIB milling of trenches, at various stages of conversion: a) a chitinous starting scale, b) an as-coated scale after 51 SSG deposition cycles, c) a SSG coated scale after organic pyrolysis, and d) a SSG coated and pyrolyzed scale after MWHT conversion into BaTiO₃. Scale bars: 1 μm.

Table 1: Dimensional measurements at various stages of conversion^[a]

Process step →	Chitin scales	As SSG coated	After pyrolysis	After MWHT treatment
Feature ↓				
ridge spacing [nm] ^[b]	2230 ± 140	2240 ± 120	1690 ± 120	1880 ± 200
strut width [nm] ^[b]	205 ± 30	270 ± 50	180 ± 30	360 ± 60

[a] See Supporting Information for discussion of statistical analyses.

[b] See Figure 1a for illustration of ridge spacing and strut width.

cantly after such firing (Table 1; Figure 1c vs. 1b). However, such shrinkage did not result in complete collapse of the hollow cores, as revealed in Figure S1c. The remarkable retention of the 3D butterfly scale morphology in the chitin-free hollow titania structures (both after oxygen plasma treatment and thermal pyrolysis) indicated that the thin SSG coating was rigid and highly interconnected. After MWHT conversion, the hollow cores of the titania structures had become largely filled by barium titanate (compare Figures S1d and S1c) and an increase in the average strut width was detected (Table 1, Figure 1d vs. 1c; Figure 4d vs. 4c, Figure S2b vs. S2a). Such strut filling and swelling was not surprising, given the increase in molar volume associated with the conversion of titania into barium titanate (i.e., the molar volumes of anatase TiO₂ and tetragonal BaTiO₃ are 20.5 and 38.8 cm³ mol⁻¹, respectively^[7]). The preservation of the overall 3D TiO₂ (and butterfly scale) morphology by the BaTiO₃-converted specimens was consistent with BaTiO₃ formation occurring largely on the surfaces of the interconnected TiO₂ particles through an in situ transformation mechanism or a dissolution–heterogeneous precipitation mechanism reported by several authors.^[8]

In summary, intricate 3D bioorganic templates (*Morpho helenor* butterfly wing scales) have been converted into multi-

component oxide (tetragonal BaTiO₃) structures that retained the 3D template morphology and micro-to-nano-scale features by combined use of a layer-by-layer conformal coating (SSG) process and modest temperature hydrothermal (MWHT) reaction process. This general approach may be applied to other bioorganic templates, or to synthetic organic templates, with multifarious 3D morphologies, provided such templates possess (or can be functionalized to possess)^[2c] a high surface coverage of hydroxy groups for SSG processing. Given the extensive variety of commercial alkoxides available for sol–gel processing, and the capability for low-temperature hydrothermal reaction into numerous ceramic compounds,^[3] this process may be used to convert organic templates (of biological or synthetic origin) into functional multicomponent ceramic materials with a wide variety of compositions, 3D structures, and properties.

Experimental Section

Butterfly wing scales were exposed to 51 SSG cycles by use of a computer-controlled deposition system.^[2c,d] Each exposure cycle consisted of immersion in a solution of 0.05 M titanium(IV) isopropoxide in isopropyl alcohol (IPA) for 10 min, washing with anhydrous IPA, immersion in a solution of 40 vol % IPA in water for 3 min, washing with anhydrous IPA, and then drying with a stream of flowing nitrogen at room temperature. Organic pyrolysis was conducted by heating the coated scales at 0.5 °C min⁻¹ to 450 °C and holding at this temperature for 4 h in air. The pyrolyzed scales were placed in vessels (TFM-lined XP-1500 Plus, CEM Corp., Matthews, NC, USA) containing a solution of 0.125 M barium acetate and 1 M sodium hydroxide dissolved in previously boiled water. The sealed specimens were then heated to 220 °C in a microwave reaction system (MARS 230/60, 2.45 GHz, CEM Corp.) and held at this temperature for 10 h to allow for MWHT conversion into barium titanate. Additional experimental details, a schematic of the overall process, and Figures S1 and S2 are provided in the Supporting Information.

Received: May 25, 2010

Revised: June 16, 2010

Published online: September 8, 2010

Keywords: barium titanate · biological templates · hydrothermal synthesis · sol–gel processes · three-dimensional replicas

- [1] a) K. H. Sandhage, M. B. Dickerson, P. M. Huseman, M. A. Caranna, J. D. Clifton, T. A. Bull, T. J. Heibel, W. R. Overton, M. E. A. Schoenwaelder, *Adv. Mater.* **2002**, *14*, 429–433; b) K. H. Sandhage, R. L. Snyder, G. Ahmad, S. M. Allan, Y. Cai, M. B. Dickerson, C. S. Gaddis, M. S. Haluska, S. Shian, M. R. Weatherspoon, R. A. Rapp, R. R. Unocic, F. M. Zalar, Y. Zhang, M. Hildebrand, B. P. Palenik, *Int. J. Appl. Ceram. Technol.* **2005**, *2*, 317–326; c) J. Zhao, C. S. Gaddis, Y. Cai, K. H. Sandhage, *J. Mater. Res.* **2005**, *20*, 282–287; d) Y. Cai, S. M. Allan, F. M. Zalar, K. H. Sandhage, *J. Am. Ceram. Soc.* **2005**, *88*, 2005–2010; e) J. C. Lytle, N. R. Denny, R. T. Turgeon, A. Stein, *Adv. Mater.* **2007**, *19*, 3682–3686.
- [2] a) I. Ichinose, H. Senzu, T. Kunitake, *Chem. Lett.* **1996**, *10*, 831–832; b) I. Ichinose, H. Senzu, T. Kunitake, *Chem. Mater.* **1997**, *9*, 1296–1298; c) M. R. Weatherspoon, M. B. Dickerson, G. Wang, Y. Cai, S. Shian, S. C. Jones, S. R. Marder, K. H. Sandhage, *Angew. Chem.* **2007**, *119*, 5826–5829; *Angew. Chem. Int. Ed.* **2007**, *46*, 5724–5727; d) M. R. Weatherspoon, Y. Cai, M. Crne, M.

- Srinivasarao, K. H. Sandhage, *Angew. Chem.* **2008**, *120*, 8039–8041; *Angew. Chem. Int. Ed.* **2008**, *47*, 7921–7923.
- [3] a) S. Komarneni, Q. Li, K. Stefansson, R. Roy, *J. Mater. Res.* **1993**, *8*, 3176–3183; b) W. Sun, C. Li, J. Li, W. Liu, *Mater. Chem. Phys.* **2006**, *97*, 481–487.
- [4] a) M. Srinivasarao, *Chem. Rev.* **1999**, *99*, 1935–1961; b) P. Vukusic, J. R. Sambles, *Nature* **2003**, *424*, 852–855; c) J. D. Schiffman, C. L. Schauer, *Mater. Sci. Eng. C* **2009**, *29*, 1370–1374.
- [5] a) G. Haertling, *J. Am. Ceram. Soc.* **1999**, *82*, 797–818; b) S. Pann, N. Alford in *Handbook of Low and High Dielectric Constant Materials and Their Applications*, Vol. 2 (Ed.: H. S. Nalwa), Academic Press, San Diego, **1999**, pp. 493–522; c) V. R. W. Amarakoon, B. C. LaCourse, O. Hernandez, J. G. Fagan, J. Pietras, J. L. Peterson, *Ceram. Trans.* **1995**, *49*, 15–26.
- [6] a) U. Balachandran, N. G. Eror, *J. Solid State Chem.* **1982**, *42*, 276–282; b) C. H. Perry, D. B. Hall, *Phys. Rev. Lett.* **1965**, *15*, 700–702.
- [7] Powder Diffraction File Card No. 00-021-1272 for anatase TiO₂, Card No. 00-005-0626 for tetragonal BaTiO₃, International Center on Diffraction Data, Newtown Square, PA, USA.
- [8] a) N. A. Ovramenko, L. I. Shvets, F. D. Ovcharenko, B. Y. Kornilovich, *Izv. Akad. Nauk SSSR Neorg. Mater.* **1979**, *15*, 1982–1985; b) W. Hertl, *J. Am. Ceram. Soc.* **1988**, *71*, 879–883; c) J. Eckert, C. Hung-Houston, B. Gersten, M. Lencka, R. Riman, *J. Am. Ceram. Soc.* **1996**, *79*, 2929–2939.